



Proceedings of the Sixth International Conference on  
Railway Technology: Research, Development and Maintenance  
Edited by: J. Pombo  
Civil-Comp Conferences, Volume 7, Paper 7.11  
Civil-Comp Press, Edinburgh, United Kingdom, 2024  
ISSN: 2753-3239, doi: 10.4203/ccc.7.7.11  
©Civil-Comp Ltd, Edinburgh, UK, 2024

# **Multiple Wheel Flat Identification in a Freight Train Through Track-Side Monitoring System**

**M. Mohammadi<sup>1</sup>, A. Mosleh<sup>1</sup>, C. Vale<sup>1</sup>, D. Ribeiro<sup>2</sup>,  
P. A. Montenegro<sup>1</sup> and A. Meixedo<sup>1</sup>**

**<sup>1</sup>CONSTRUCT-LESE, Faculty of Engineering, University of  
Porto, Porto, Portugal**

**<sup>2</sup> CONSTRUCT, School of Engineering, Polytechnic of Porto  
Porto, Portugal**

## **Abstract**

Wheel flat defect is the most common type of damage on train wheels, which can cause a high impact on the railway infrastructure and vehicle components. Artificial intelligence techniques for detecting geometric defects in train wheels have significantly enhanced railway maintenance and safety efficiency. Artificial intelligence systems excel in analyzing intricate wheel rotation patterns, swiftly and accurately identifying potential geometric deformations that could lead to wheel flats. Compared to traditional methods, artificial intelligence-driven defect identification provides a faster and more reliable approach, ensuring the safety and reliability of railway operations. This study proposes a discrimination learning algorithm to identify railway wheel flats, which consists of two stages: i) wheel flat detection to distinguish a healthy wheel from a damaged one; ii) classification of wheel damage based on its severity. To validate the unsupervised learning method, synthetic data acquired from a virtual wayside monitoring system is used, considering freight train passages, including wheels afflicted by single or multiple defects. The developed methodology in this study represents effectiveness in detecting wheel flats and assessing the damage severity, regardless of the number of defective wheels.

**Keywords:** wheel flat detection, wayside condition monitoring, train-track interaction, damage classification, unsupervised learning, machine learning.

# 1 Introduction

Continuous operation of trains with damaged wheels increases the risk of track misalignment, which can potentially lead to derailments. Additionally, the ongoing effects of these defective wheels can cause structural damage to railway vehicles and their components over time, jeopardizing their integrity and lifespan. Therefore, it's crucial to regularly monitor the geometric quality of wheels on all railway vehicles to identify potential defects and classify their severity. Particular consideration should be given to freight trains due to their heavy loads and frequent use, making them more susceptible to wheel-related conditions [1].

It is foreseen that there will be a substantial shift in the transportation of goods from road to rail in the near future. As a result, in the absence of a safe rail transport system, increasing demand for the use of rail transport potentially results in derailments and disruptions in railway operations caused by defects in freight trains. Therefore, there is a vital need for innovative approaches to monitoring wheel conditions, including automatic detection and classification of out-of-roundness (OOR) wheels. OOR defects can cause vibrations that can damage the track and the vehicle components [2]. There are various types of OOR defects, including flats, eccentricities, polygons, corrugations on block-braked wheel treads, missing pieces of tread material due to fatigue cracking, and other random irregularities [3-5]. Among these, wheel flats are a frequently encountered form of wheel damage resulting from the friction between the wheel and rail caused by braking forces. This friction can remodel the wheel's exterior perimeter from round to flat [6].

The identification of defective wheels can be accomplished through the measurements obtained from wayside or onboard monitoring systems. As per the onboard methods, sensors are required on each vehicle wheel to evaluate their condition, resulting in a substantial cost for the monitoring system [7, 8]. To address this issue, wayside measurement systems are currently the most preferred solution for detecting flat wheels, as they can monitor the wheels of various vehicles as they pass through specific locations along the track [6]. Various sensors can be employed for the detection of wheel flats, including fiber Bragg gratings [9], acoustic emission sensors [10], strain gauges [11, 12], and accelerometers [6, 11, 13].

Different methods for automatic detection are employed to enhance result reliability, with the integration of more advanced techniques on a regular basis. Mosleh et al. [14] developed a method using the envelope spectrum to differentiate between defective and healthy wheels, which proved effective for polygonal wheels [13]. Chen et al. [15] developed a two-level adaptive chirp mode decomposition (ACMD) approach for wheel flat detection based on vehicle vibration measurements. Nowakowski et al. [16] proposed an approach involving vibration signal processing in the frequency and time domain to identify wheel flats.

In recent years, the application of machine learning (ML) techniques has become increasingly prevalent in the detection of damage in vehicle systems. Dernbakh et al. [17] developed various classifier methods, including support vector machine (SVM)

and standard convolutional network (CNN), to identify wheel flats. Qing Ni et al. [18] devised a Bayesian machine learning technique for detecting train wheel damage and assessing wheel condition, which comes with more accurate responses compared to offline methods. Moreover, Mosleh et al. [1] developed an unsupervised detection methodology that automatically distinguishes between defective and healthy wheels based on acceleration and shear time histories evaluated on the rails. Afterward, Mohammadi et al. [6] proposed a discrimination learning approach for detecting wheel flat based on rail acceleration measurements to compare the accuracy of the different feature extraction techniques in wheel flat detection.

However, it is notable that none of the prior studies on wheel flat detection have advanced to the point of classifying damage on vehicle wheelsets using wayside monitoring systems that include train passages with single and multi-damaged wheels. The aim of this study is to detect wheel flats and classify damage severity into three levels: low, moderate, and severe, regardless of the number or position of the wheel flat. An artificial wayside monitoring system is employed to validate the proposed methodology, and numerical simulations are carried out to evaluate its effectiveness.

## **2 Numerical simulation**

This section represents the numerical simulations of vehicle, track, and irregularity. Moreover, the description of the wheel flat profile, dynamic train-track interaction, and damaged and undamaged train scenarios are described.

### **2.1 Train-track interaction**

The Laagrss freight train comprising five wagons is considered as a vehicle model to be evaluated in the current research. According to the UIC classification [19], the train can reach a maximum speed of 120 km/h, a tare weight of 27 t, and a load capacity of 52 t. To simulate suspensions in all directions, a 3-D multibody dynamic model is computed using ANSYS® [20]. This model incorporates spring-damper and mass-point elements to accurately represent the mass and inertia at the center of gravity of each wagon component. Furthermore, the different components are connected by rigid beams. All train components' geometric and mechanical properties are described in Bragança et al.'s work [21].

Additionally, the finite element model of the track is developed in ANSYS® [20] and validated by Montenegro et al. [22]. The model of the track is employed through a multi-layer scheme to simulate ballast, sleepers, and rails. The rail pads between the sleepers and the rail are simulated as connecting spring elements. Beam elements are used to represent the rails and sleepers, with appropriate material properties assigned to each. The ballast, on the other hand, is represented by discrete mass points. Spring dashpot elements are also incorporated to consider the flexibility of the foundation. Further details on the track model are mentioned in the work of Mosleh et al. [14].

In real terms, Imperfections can be observed in the rails under track conditions. Despite their small size, these irregularities have a notable effect on the contact between the wheel and rail [23]. Hence, rail unevenness profiles are generated within

the wavelength intervals D1 and D2, which correspond to wavelengths ranging from 1 m to 75 m as defined in European Standard EN 13848-2 [24]. Moreover, PSD curves are developed using real data to produce synthetic unevenness profiles. Mosleh et al. [25] provide more detail on the generation process of rail unevenness profiles.

To simulate the dynamic interactions between trains and tracks, the authors have developed an in-house software called VSI - Vehicle-Structure Interaction Analysis. This software has been validated and extensively described in previous publications [26] and used in various applications [11, 22]. The calculation of normal contact forces is based on Hertzian theory using a 3D wheel-rail contact model, while the USETAB routine is utilized to determine tangential forces resulting from rolling friction creep. MATLAB<sup>®</sup> [27] is used as a numerical tool to import the structural matrices of both vehicles and tracks, which were previously modeled using finite element analysis (FE). Both subsystems are initially modeled in ANSYS<sup>®</sup> [20] separately and then integrated using the VSI software in a fully coupled manner [26]. The authors' previous publications [14] describe train-track interaction in more detail. Figure 1 presents the numerical model. wheel flat identification is performed using eight accelerometers along the track (four sensors on each side), positioned on the rail between two sleepers.

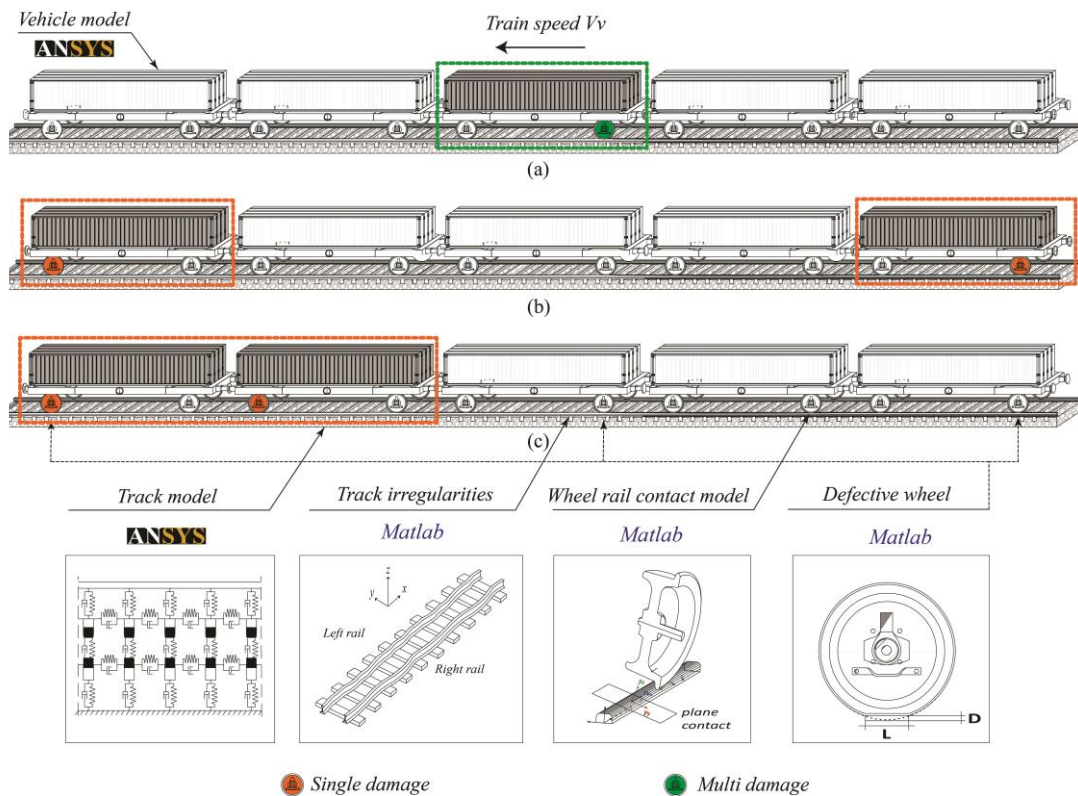


Figure 1. Dynamic train-track interaction numerical simulation.

The various severities of wheel flats are considered to simulate defective wheels on a train. The categorization of wheel flats into low, moderate, and severe is based on the length of the flats ( $L$ ). The lower and upper limits for the wheel's flat length in

each interval are determined by the uniform distributions  $U(10, 20)$ ,  $U(25, 50)$ , and  $U(55, 100)$ , respectively. The computation of the wheel flat depth ( $D$ ) is done using the equation:

$$D = \frac{L^2}{16R_w} \quad (1)$$

The radius of the wheel is denoted by  $R_w$ , while the length of the flat length is represented by  $L$ . Additionally, the vertical profile of a wheel flat is determined using the following formula:

$$Z = -\frac{D}{2} \left( 1 - \cos \frac{2\pi x}{L} \right) \cdot H(x - (2\pi R_w - L)), \quad 0 \leq x \leq 2\pi R_w \quad (2)$$

In which,  $x$  represents the coordinate aligned with the track's longitudinal direction, and  $H$  is the Heaviside periodic function.

## 2.2 Damaged and undamaged scenarios

To evaluate the automatic wheel flat identification method developed in this study, both undamaged and damaged train passage scenarios are simulated. The undamaged scenario depicts the train passing with wheels in normal condition, while the damaged scenario represents a train passing with defective wheels. Figure 1 illustrates three different cases of damaged layouts, including a single-damage scenario where the left wheel of the rear wheelset of the third wagon is flat and highlighted in green (Figure 1a). Additionally, the far multi-damage scenarios with defects on the left wheel of the rear wheelset of the first wagon and the left wheel of the front wheelset of the last wagon are illustrated in orange (Figure 1b). Furthermore, the near multi-damage scenarios are also shown with flats in the left wheel of the rear wheels of the first and second wagons, highlighted in orange (Figure 1c).

For the baseline scenario, a total of 113 simulations were conducted, as illustrated in Table 1. Four different rail unevenness profiles, five varying train speeds (ranging from 40 to 120 km/h), and six loading schemes: (i) empty train; (ii) half-loaded train; (iii) three fully loaded trains with longitudinal and transversal unbalanced loads (UNB1, UNB2, and UNB3) are considered. The unbalanced loading configurations for the wagon model were determined according to the UIC loading guidelines [10], which involve offsetting the cargo gravity center in both longitudinal and transversal directions.

	<b>Baseline scenario</b>	<b>Damaged scenario</b>
Train	Freight – Laagrss wagon	
Number of loading schemes	6	1 (full capacity)
Unevenness profiles	4	1
Speeds (km/h)	40 – 120	80
Noise ratio	5%	
Flat lengths (mm)	-	10-20 mm (L1) 25-50 mm (L2) 55-100 mm (L3)
<b>Number of numerical analysis</b>	113	42

Table 1: Defective and healthy train scenarios.

A total of 42 scenarios are modeled, each featuring distinct flat geometries while the train is passing at a speed of 80 km/h (as depicted in Figure 8). 30 simulations including the train passing with a single damaged wheel while the remaining 12 simulations involve cases with multiple damages. For the single damage scenario, 30 analyses are conducted, simulating 10 analyses for each flat length interval (low, moderate, and severe).

In the case of multi-damage scenarios, a total of 12 analyses are conducted. Among these analyses, six simulations include two defective wheels with identical severities (low-low, moderate-moderate, and severe-severe) for both the first and second wagons (train passages 31, 32, and 33), classified as far-multi-damage (Figure 1b) and for the first and last wagons (simulations 37, 38, and 39), referred to as near-multi-damage (Figure 1c). Furthermore, the remaining six analyses involve two defective wheels with varying severities, such as low and moderate, low and severe, and moderate and severe flat properties (train passages 34, 35, and 36), for both the first and last wagons (Figure 1b), as well as for the first and second wagons in simulations 40, 41, and 42 (Figure 1c).

The evaluation of acceleration signals in baseline and damaged scenarios is conducted using a sampling frequency of 10 kHz, along with the artificial noise (5% amplitude), to simulate real-world conditions for the measured rail response. Additionally, a low-pass Chebyshev type II digital filter with a cut-off frequency of 500 Hz is applied to filter the time-series data.

### **3 Proposed methodology for automatic wheel flat identification**

As illustrated In Figure 2, the automatic wheel flat identification process developed in this research consists of two stages. In the first stage, a confidence boundary is established by analyzing the baseline responses of the rail to detect train passages with defective wheels. The second stage enables the classification of a wheel flat based on

the damage severity. All the steps of this procedure are summarized in the flowchart presented in Figure 1. The automatic wheel flat detection includes five steps in the first stage as follows:

- 1- The input signals are captured using installed sensors on the rail.
- 2- Feature extraction from multiple sensors is accomplished through the implementation of the Continuous wavelength transform (CWT). This transformative process converts time series measurements into damage-sensitive features while simultaneously achieving notable data compression.
- 3- In order to suppress environmental and operational effects and enhance their sensitivity to damage, Principal Component Analysis (PCA) is applied to the extracted features.
- 4- Furthermore, the application of the Mahalanobis distance enhances the sensitivity of the modeled features. The fusion of each sensor's features is effectively accomplished through the Mahalanobis distance. A damage indicator (DI) is produced for each train passage.
- 5- An assessment of a wheel's condition is conducted through a statistical method to differentiate between a healthy and defective state. The estimation of a statistical confidence boundary (CB) is derived from a Gaussian Inverse Cumulative Distribution Function.

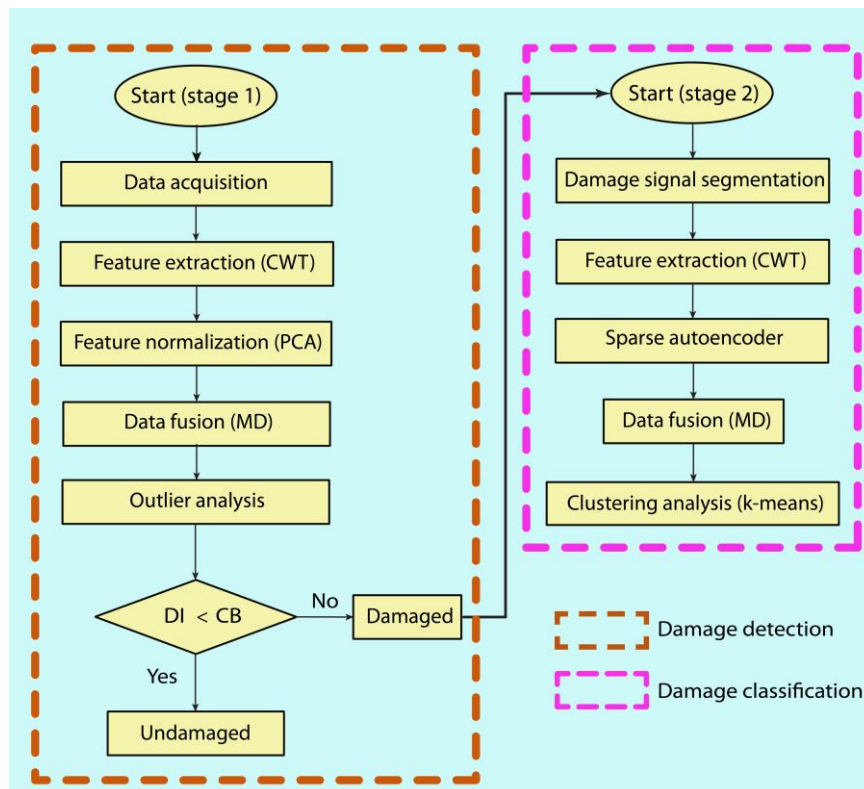


Figure 2. The framework of wheel flat identification.

After detecting the train passages, including defective wheels, the healthy scenarios are discarded in the second stage. subsequently, the detected signals corresponding to the defective scenarios are used as input for damage severity classification in the second stage. The proposed methodology classifies the damage severity through the following five steps:

- 1- Initially, the signals are segmented for both single and multi-damaged scenarios using an automatic segmentation technique [28]. The main purpose of this step is to separate the signal corresponding to each defective wheel in multi-damage scenarios.
- 2- Afterward, the damage-sensitive features are extracted using CWT using the cut signal.
- 3- The Sparse autoencoder is implemented to obtain alternative features by computing Mean Squared Error (MSE) and Mean Absolute Error (MAE) between original CWT-based features.
- 4- Furthermore, MD is calculated using MSE and MAE to enhance sensitivity to the damage.
- 5- Finally, the severity of the defect is classified using the *K*-means clustering technique.

## **4 Results**

This research's output is divided into two distinct sections. Initially, the study detects defective wheels from healthy ones and then classifies the damage based on the severity of the defects.

### **4.1 Wheel flat detection**

As described in Figure 2, wheel flat detection includes 4 main steps after data acquisition. The output of each step, namely feature extraction, feature normalization, data fusion, and damage detection, are represented in this section separately.

#### **4.1.1 Feature extraction**

A total of 468 features are computed using time series data for each accelerometer. The analysis consists of a total of 155 simulations, which include both baseline and damaged scenarios. By applying the Continuous Wavelet Transform (CWT) to signals of these scenarios, a three-dimensional matrix of size 155-by-468-by-8 for each of the eight measurement points is obtained. Figure 3 represents four of the 468 CWT features based on the measured accelerations. The features can be categorized into two main groups based on the condition of the train's wheels: baseline scenarios (first 113 passages) and damaged scenarios (42 passages following the occurrence of damage). Each single damage scenario is represented by ten symbols, which correspond to different levels of wheel flat severity ranging from low to severe damage. Consequently, simulations 114 to 123 represent vehicle passages with low



wheel flat lengths between 10 and 20 mm (SD-low), while simulations 124 to 133 represent vehicle passages with wheel flat lengths between 25 and 50 mm (SD-moderate). In simulations 134 to 143, the range of 55 to 100 mm (SD-severe) is considered for wheel flat length. Finally, damage scenarios 144 to 155 show vehicle passages with multi-defective wheels.

The variety of information in different CWT-based damage-sensitive features is illustrated in Figure 3. Notably, Figure 3a and Figure 3b demonstrate a specific ascending sensitivity pattern for single-damaged scenarios, thereby highlighting the visible amplitude differences between low-damage scenarios and moderate to severe damage scenarios. On the contrary, Figure 3c demonstrates a steady change in amplitude, with no discernible difference between baseline and damage scenarios. On the other hand, Figure 3d illustrates an inconsistent amplitude variation. Therefore, it can be concluded that the distinction between baseline and damage scenarios is not clear due to the impact of environmental and operational factors. As a result, feature normalization is implemented in the following section.

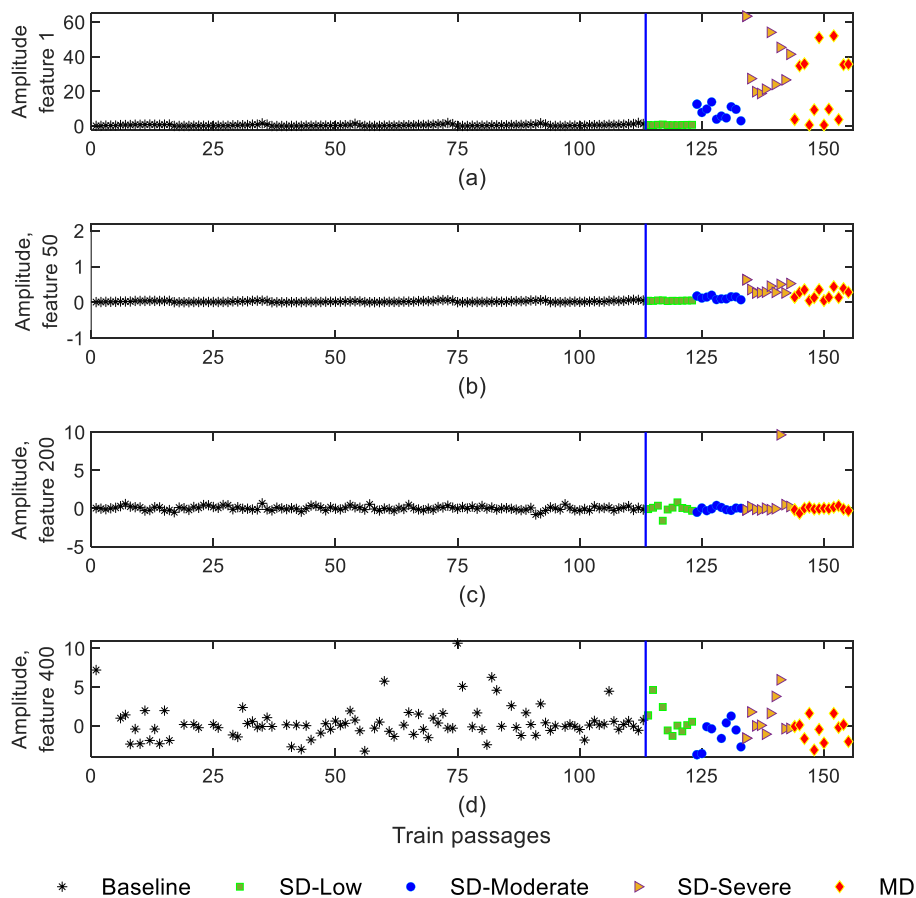


Figure 3. Feature extraction based on the CWT technique.

### 4.1.2 Feature normalization

In the second step of damage detection, the first 15 components are eliminated as the cumulative variance exceeds 80%, resulting in an 8-by-468 matrix of features generated by PCA for each vehicle passage. Figure 4 represents four normalized features, indicating the impact of EOVs on feature extraction and normalization Figures. However, distinguishing between undamaged and damaged wheels post-PCA implementation proves challenging due to minimal differences, leading to a data fusion approach discussed in the subsequent section.

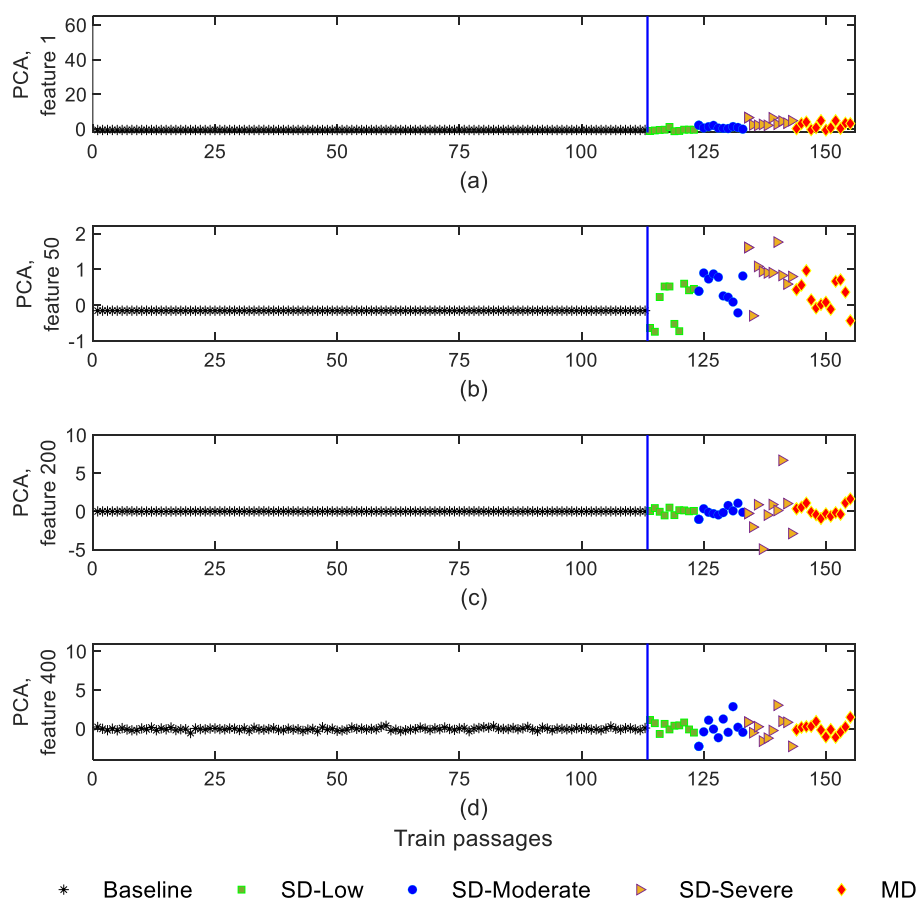


Figure 4. Feature normalization based on PCA technique.

### 4.1.3 Data fusion

Data fusion involves computing MD to obtain a damage index (DI). The application of MD allows each sensor and vehicle passage to be transformed into a damage-sensitive feature based on 453 PCA-CWT parameters. The output of this process consists of 155 by-1 vectors of Mahalanobis distances. Figure 5 represents the improved sensitivity to damage and the varying sensitivities of sensors to damage, leading to disparate damage indexes.

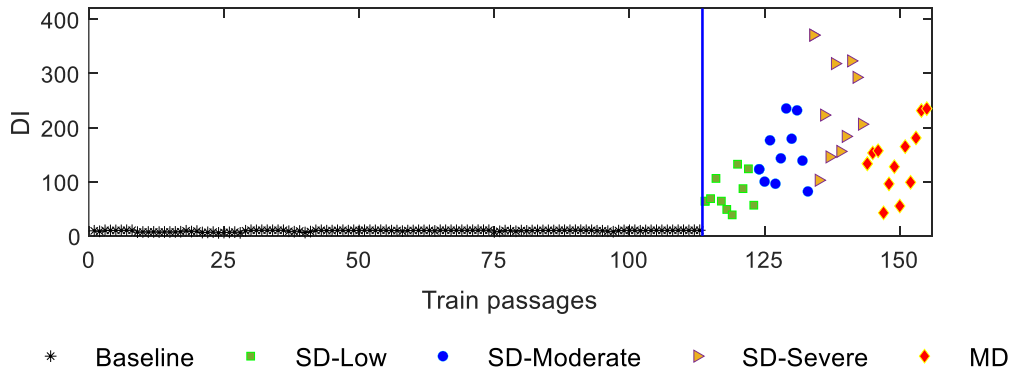


Figure 5. Data fusion based on computing Mahalanobis distance

#### 4.1.4 Detection

The first stage of the proposed approach concludes with the implementation of automatic wheel flat detection (Figure 2). This detection is accomplished using a CB calculated through a Gaussian inverse cumulative distribution function. A threshold of 1% is set as the significance level. Figure 6 illustrates the wheel flat detection considering all 155 wheel conditions. The results represented in this figure demonstrate the exceptional efficacy of the proposed method in accurately distinguishing between healthy and damaged scenarios without occurrences of false positives or false negatives.

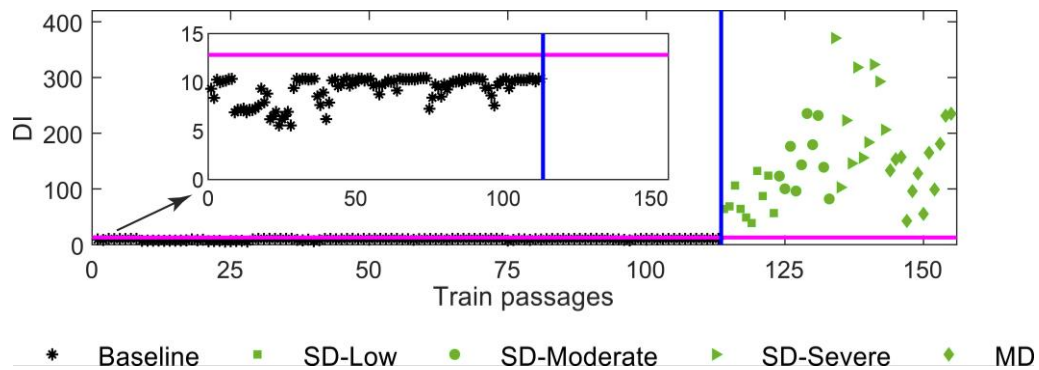


Figure 6. Automatic wheel flat detection.

#### 4.2 Wheel flat classification

Figure 7 describes the automatic classification of wheel flats based on their severity using the segmented acceleration signal. This figure illustrates the division of damaged scenarios into two sections by a blue line. The initial 30 indicators describe train passages with single defective wheels, while the remaining 24 indicators correspond to multi-damage scenarios involving two defective wheels. Each multi-

passage involves two damaged wheels; therefore, a total of 24 segmented signals are generated.

The outputs presented in Figure 7 indicate that the developed approach in the current study is capable of classifying defective wheels according to their severity (low, moderate, and severe) with just a single sensor, irrespective of whether the train has one or multiple damaged wheels. As shown in Figure 7, the damage severity classification with a single sensor results in only two misclassifications.

One of these damage indexes corresponds to the train passage, including one defective wheel with a flat length measuring 27.5 mm. This measurement comes close to the lower boundary of damage severity (10-20 mm), resulting in misclassification. On the other hand, the second misclassification occurs in train passage involving multiple damages, and the damaged wheel is located on the second wagon with a flat length of 40 mm. It can be concluded that the proposed unsupervised methodology can classify damage severities into low, moderate, and severe levels. This damage classification is achieved regardless of the number of defective wheels in each train passage.

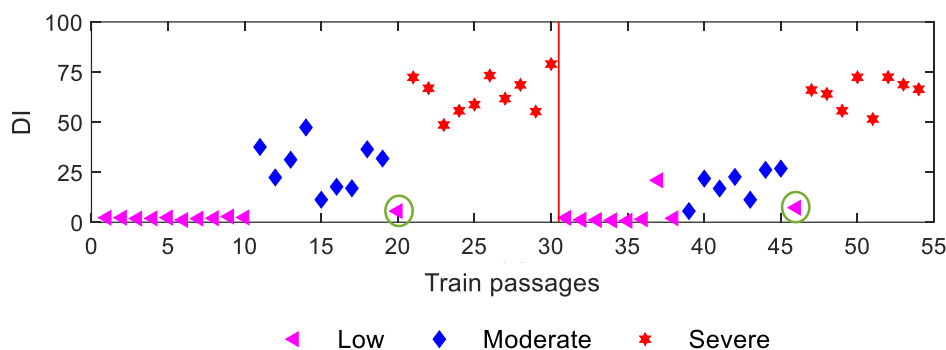


Figure 7. Wheel flat severity classification.

## 5 Conclusions

This study presents an unsupervised discrimination algorithm for wheel flat identification. It operates in two stages: first, detecting wheel flats by establishing a confidence boundary, and second, classifying wheel damage based on its severity. The algorithm's effectiveness is validated using artificial data from a virtual wayside monitoring system concerning freight train passages. The proposed methodology is capable of distinguishing train passages with defective wheels from healthy ones. Moreover, the developed algorithm automatically classifies the defect severity into low, moderate, and severe damage levels, regardless of the number or position of the defect.

## Acknowledgments

This work was financially supported by Base Funding-UIDB/04708/2020 and Programmatic Funding-UIDP/04708/ 2020 of the CONSTRUCT - Instituto de Estruturas e Construções, funded by national funds through the FCT/ MCTES (PIDDAC). The second author acknowledges Grant no. 2021.04272.CEECIND from the Stimulus of Scientific Employment, Individual Support (CEECIND) - 4rd Edition provided by “FCT – Fundação para a Ciência, DOI : 10.54499/2021.04272.CEECIND/CP1679/CT0003”.

## References

- [1] A. Mosleh, A. Meixedo, D. Ribeiro, P. Montenegro, R. Calçada, Automatic clustering-based approach for train wheels condition monitoring. *International Journal of Rail Transportation*, p. 1-26, 2022.
- [2] C. Vale, "Wheel Flats in the Dynamic Behavior of Ballasted and Slab Railway Tracks", *Applied Sciences*, 11(15): p. 7127, 2021.
- [3] Rail Industry Safety and Standards Board, "Code of Practice for Wheel Defects", 2020.
- [4] D.W. Barke, W.K. Chiu, "A review of the effects of out-of-round wheels on track and vehicle components", *Proceedings of the Institution of Mechanical Engineers, Part F: Journal of Rail and Rapid Transit*, 219(3): p. 151-175, 2005.
- [5] A. Johansson, J.C. Nielsen, "Out-of-round railway wheels wheel-rail contact forces and track response derived from field tests and numerical simulations", *Proceedings of the Institution of Mechanical Engineers, Part F: Journal of Rail and Rapid Transit*, 217(2): p. 135-146, 2003.
- [6] M. Mohammadi, A. Mosleh, C. Vale, D. Ribeiro, P. Montenegro, A. Meixedo, "An Unsupervised Learning Approach for Wayside Train Wheel Flat Detection", *Sensors*, 23(4): p. 1910, 2023.
- [7] A. Alemi, F. Corman, G. Lodewijks, "Condition monitoring approaches for the detection of railway wheel defects", *Proceedings of the Institution of Mechanical Engineers, Part F: Journal of Rail and Rapid Transit*, 231(8): p. 961-981, 2017.
- [8] N. Bosso, A. Gugliotta, N. Zampieri, "Wheel flat detection algorithm for onboard diagnostic", *Measurement*, 123: p. 193-202, 2018.
- [9] S. Mishra, P. Sharan, K. Saara, "Real time implementation of fiber Bragg grating sensor in monitoring flat wheel detection for railways", *Engineering Failure Analysis*, 138: p. 106376, 2022.
- [10] M. Aktas, E.H. Gunel, P. Yilmazer, T. Akgun, "Detection of wheel flatten defect on the moving train with acoustic emission sensor", in *2018 IEEE 29th Annual International Symposium on Personal, Indoor and Mobile Radio Communications (PIMRC)*, IEEE, 2018.
- [11] A. Mosleh, P.A. Montenegro, P.A. Costa, R. Calçada, "Railway Vehicle Wheel Flat Detection with Multiple Records Using Spectral Kurtosis Analysis", *Applied Sciences*, 11(9): p. 4002, 2021.

- [12] Z. Sun, X.-W. Ye, J. Lu, "Estimating stay cable vibration under typhoon with an explainable ensemble learning model", *Structure and Infrastructure Engineering*, p. 1-13, 2023.
- [13] V. Gonçalves, A. Mosleh, C. Vale, P.A. Montenegro, "Wheel Out-of-Roundness Detection Using an Envelope Spectrum Analysis", *Sensors*, 23(4): p. 2138, 2023.
- [14] A. Mosleh, P. Montenegro, P. Alves Costa, R. Calçada, "An approach for wheel flat detection of railway train wheels using envelope spectrum analysis", *Structure and Infrastructure Engineering*, 17(12): p. 1710-1729, 2021.
- [15] S. Chen, K. Wang, C. Chang, B. Xie, W. Zhai, "A two-level adaptive chirp mode decomposition method for the railway wheel flat detection under variable-speed conditions", *Journal of Sound and Vibration*, 498: p. 115963, 2021.
- [16] T. Nowakowski, P. Komorski, G.M. Szymański, F. Tomaszewski, "Wheel-flat detection on trams using envelope analysis with Hilbert transform", *Latin American Journal of Solids and Structures*, 16, 2019.
- [17] G. Dernbach, A. Lykartsis, L. Sievers, S. Weinzierl, "Acoustic Identification of Flat Spots On Wheels Using Different Machine Learning Techniques Gabriel Dernbach<sup>1</sup>", Athanasios Lykartsis<sup>1</sup>, Leon Sievers<sup>2</sup>, Stefan Weinzierl<sup>1</sup>, 2020.
- [18] Y.-Q. Ni, Q.-H. Zhang, "A Bayesian machine learning approach for online detection of railway wheel defects using track-side monitoring. *Structural Health Monitoring*, 20(4): p. 1536-1550, 2021.
- [19] UIC, "Code of practice for the loading and securing of goods on railway wagons", Paris, 2022.
- [20] ANSYS<sup>®</sup>, Canonsburg, PA, USA: Academic Research, Release 19.2, 2018.
- [21] C. Bragança, J. Neto, N. Pinto, P.A. Montenegro, D. Ribeiro, H. Carvalho, R. Calçada, "Calibration and validation of a freight wagon dynamic model in operating conditions based on limited experimental data", *Vehicle System Dynamics*, 60(9): p. 3024-3050, 2022.
- [22] P.A. Montenegro, R. Heleno, H. Carvalho, R. Calçada, C.J. Baker, "A comparative study on the running safety of trains subjected to crosswinds simulated with different wind models", *Journal of Wind Engineering and Industrial Aerodynamics*, 207: p. 104398, 2020.
- [23] V.C.C. R., "Dynamic Response of a Coupled Vehicle-Track System to Real Longitudinal Rail Profiles", in *Proceedings of the Tenth International Conference on Computational Structures Technology*, Civil-Comp Press, Stirlingshire, UK, 2010.
- [24] E. STANDARD, "Railway applications - Track - Track geometry quality - Part 2: Measuring systems - Track recording vehicles (EN 13848-2)", Brussels: EUROPEAN COMMITTEE FOR STANDARDIZATION, 2006.
- [25] A. Mosleh, P.A. Costa, R. Calçada, "A new strategy to estimate static loads for the dynamic weighing in motion of railway vehicles", *Proceedings of the Institution of Mechanical Engineers, Part F: Journal of Rail and Rapid Transit*, 234(2): p. 183-200, 2019.

- [26] P.A. Montenegro, S.G.M. Neves, R. Calçada, M. Tanabe, M. Sogabe, "Wheel rail contact formulation for analyzing the lateral train–structure dynamic interaction.", *Computers & Structures*, 152: p. 200-214, 2015.
- [27] MATLAB<sup>®</sup>, Version R2022a. Natick, Massachusetts: The MathWorks Inc, 2022.
- [28] A. Lourenço, C. Ferraz, D. Ribeiro, A. Mosleh, P. Montenegro, C. Vale, A. Meixedo, G. Marreiros, "Adaptive time series representation for out-of-round railway wheels fault diagnosis in wayside monitoring", *Engineering Failure Analysis*, 152: p. 107433, 2023.